ISSN 1063-7834, Physics of the Solid State, 2013, Vol. 55, No. 11, pp. 2311–2316. © Pleiades Publishing, Ltd., 2013.
Original Russian Text © V.A. Vazhenin, A.P. Potapov, A.V. Fokin, M.Yu. Artyomov, 2013, published in Fizika Tverdogo Tela, 2013, Vol. 55, No. 11, pp. 2196–2201.

IMPURITY CENTERS

Dimer Paramagnetic Centers in Lead Germanate Crystals Doped with Iron and Halogen (Cl^-, Br^-, F^-) Ions

V. A. Vazhenin[a], *, A. P. Potapov, A. V. Fokin, and M. Yu. Artyomov

Institute of Physics and Applied Mathematics, Ural Federal University named after the First President of Russia B.N. Yeltsin, pr. Lenina 51, Yekaterinburg, 620083 Russia

** e-mail: Vladimir.vazhenin@usu.ru*

Received April 17, 2013

Abstract—The dimer complexes Fe^{3+}–Cl^-, Fe^{3+}–Br^-, and Fe^{3+}–O^{2-} in ferroelectric lead germanate crystals doped with iron and annealed in chlorine-, bromine-, and fluorine-containing atmospheres have been studied using the electron paramagnetic resonance method. These complexes are formed by Fe^{3+} ions in the trigonal position of lead and their associated anions located in the interstitial channel of the structure. The positions of the charge-compensating anions in the channel have been discussed based on the analysis of the parameters of the spin Hamiltonian and their temperature dependence.

DOI: 10.1134/S1063783413110309

1. Electron paramagnetic resonance (EPR) of trigonal Fe^{3+} centers (the ground state $^6S_{5/2}$) in ferroelectric lead germanate was studied in [1–3]. As a result, it was concluded that these centers are associated with individual trivalent iron ions localized in the position Pb7 (in the notation of [4]) of the ferroelectric phase $Pb_5Ge_3O_{11}$. The local symmetry of the center increases in the paraelectric phase: $C_3 \longrightarrow C_{3h}$. It was found in [5] that annealing of the above crystals in chlorine-containing atmosphere leads to the appearance of several Fe^{3+}–Cl^- dimer complexes with triclinic symmetry, so that the chlorine ions are situated in the interstices of the channel (Fig. 1) formed by the Pb triangles and running along the C_3 axis [4, 6]. This work is devoted to studying the mechanisms of the formation of defects under doping of lead germanate by various halogen ions.

2. The measurements were performed on poly- and single-domain samples of $Pb_5Ge_3O_{11}$ single crystals grown with the use of the Czochralski method from the charge produced by solid-phase synthesis and doped with 0.01–0.2 mol % Fe. The second-order ferroelectric transition $P3(C_3^1) \longleftrightarrow P\bar{6}\,(C_{3h}^1)$ in pure lead germanate occurs at a temperature of 450 K [7]; its crystalline structure at room temperature and at 473 K was found in [4, 6] by neutron diffraction. To dope the crystals by halogen ions the samples were annealed at 800 K in the corresponding atmosphere for two hours. To prepare the chlorine-, bromine-, and fluorine-containing atmospheres in an open bulb we used $ZnCl_2$, CsBr, and polytetrafluoroethylene (teflon), respectively. The samples were made single-domain by cooling them down from 450 K in an electric field of 150 V/mm. The measurements were carried out on a Bruker EMX Plus X-band EPR spectrometer in the temperature range of 100–500 K.

3. The EPR spectra in the region of the high-field transition $5 \longleftrightarrow 6$ (or $1/2 \longleftrightarrow 3/2$, see Fig. 1 in [5]) of the Fe^{3+} trigonal center in the initial and annealed $Pb_5Ge_3O_{11}$ samples at room temperature in the magnetic field $\mathbf{B} \parallel C_3$ are shown in Fig. 2. Annealing in the presence of zinc chloride (spectrum *b* in Fig. 2) leads to a considerable increase in the intensity of three satellites (marked by vertical arrows). In [5], these satellites were attributed to the transitions of Fe^{3+}–Cl^- dimer complexes. It should be mentioned that the number of nonequivalent Fe^{3+}–Cl^- centers is actually more than 3, as indicated, e.g., by an increase in the line width of the trigonal complex, but we did not manage to resolve all of them. The presence of these centers in the initial crystal is caused by a small chloride contamination of germanium dioxide used in the charge synthesis.

The temperature behavior of the positions of the signals in spectrum *b* (Fig. 2) is shown in Fig. 3. It proved impossible to measure the temperature dependence for two satellites in the entire range owing to their overlap and strong (almost an order of magnitude) broadening at high temperatures. The bend in the temperature dependences near 435 K is caused by the ferroelectric transition, whose temperature is somewhat lower than 450 K owing to the presence of impurities in the crystal.

In addition to the results of [5], we measured the angular dependences of the positions of the satellites near the low-field transition $5 \longleftrightarrow 6$ (or $1/2 \longleftrightarrow -1/2$, see Fig. 1 in [5]) in the *ZX* and *ZY* planes. The following reference frame was used: $Z \parallel C_3$, the *X* axis is orthogonal to the side facet of the hexagonal prismatic

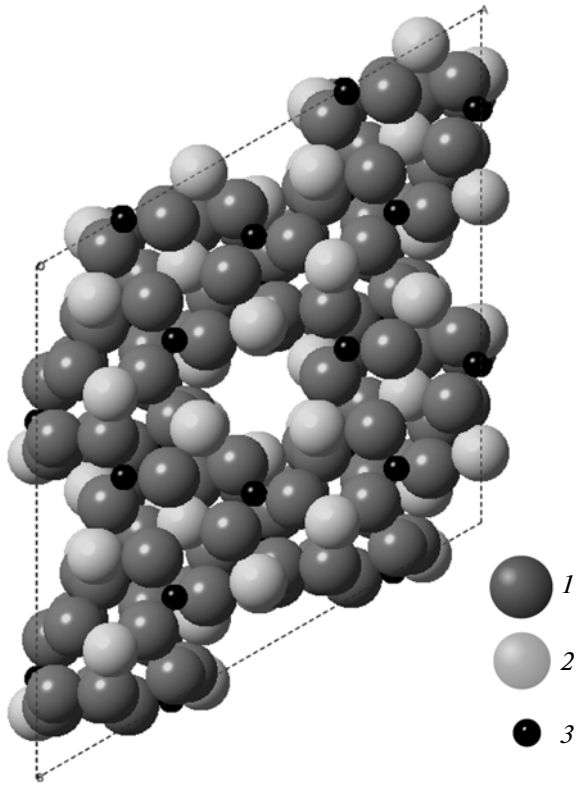

Fig. 1. View of the structure of $Pb_5Ge_3O_{11}$ along the C_3 axis: (*1*) O^{2-}, (*2*) Pb^{2+}, and (*3*) Ge^{4+}; the interstitial channel is situated at the touching point of four unit cells.

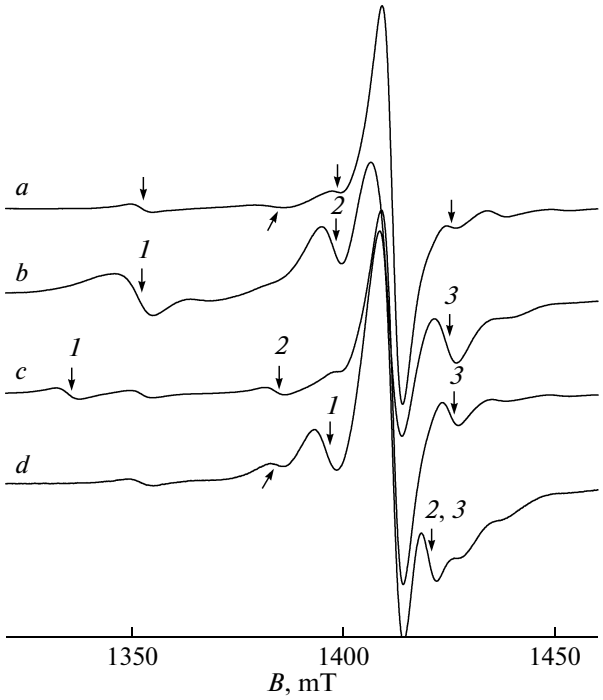

Fig. 2. EPR spectrum (absorption signal derivative) of the region of the high-field 5 ⟷ 6 transition of the nonlocally compensated Fe^{3+} ion (0.2 mol %) in $\mathbf{B} \parallel \mathbf{C}_3$ at room temperature for (*a*) initial sample, (*b*) after annealing with $ZnCl_2$, (*c*) after annealing in the bromine-containing atmosphere, and (*d*) after annealing with teflon. Arrows indicate the signals discussed in the text. The numbers of the signals correspond to the numbers of complexes in Tables 1–3.

crystal. We used the spin Hamiltonian (according to the definition [8])

$$H_{sp} = \mathbf{g}\beta(\mathbf{BS}) + \frac{1}{3}\sum_m (b_{2m}O_{2m} + c_{2m}\Omega_{2m}) + \frac{1}{60}\sum_m (b_{4m}O_{4m} + c_{4m}\Omega_{4m}), \quad (1)$$

where $\mathbf{g}$ is the g tensor, β is the Bohr magneton, $\mathbf{B}$ is the magnetic field induction, $\mathbf{S}$ is the operator of the electron spin, b_{nm} and c_{nm} are fine-structure parameters, and O_{nm} and Ω_{nm} are the cosine and sine Stevens spin operators. It was found by optimizing the parameters of Hamiltonian (1) with the use of a more extensive experimental data, as compared to [5], that the orientation behavior of the spectra of three Fe^{3+}–Cl^- complexes can be described to the same accuracy without the use of the fourth-rank fine-structure tensor (Table 1).

The quantity $b_{22\max}$ given in Table 1 determines the amplitude of the azimuthal angular dependence of the position of the transitions in $\mathbf{B} \perp \mathbf{C}_3$ being the maximum value of the parameter b_{22} under rotation of the reference frame about the Z axis; at this point, the parameter c_{22} vanishes. Inclusion of the parameter $b_{22\max}$ is explained by the fact that b_{22} and c_{22} naturally take absolutely different values for three equivalent complexes. In particular, a considerable discrepancy in the values of b_{22} and c_{22} of the complex C(Cl)-2 in Table 1 and in [5] is caused by the transition to the other equivalent center, whose azimuthal angular dependence is shifted by 60° (see Fig. 7 in [5]); in this case, $b_{22\max}$ remained almost unchanged: 1475 vs. 1470 MHz. Consequently, $b_{22\max}$ is the common characteristic of all three equivalent complexes. A difference of tens of degrees in the position of extremes of the angular dependences of nonequivalent centers (see Figs. 5 and 7 in [5]) makes impossible the attribution of the observed spectra to the complexes with the charge-compensating effect in certain channels of the structure.

As a result of annealing the $Pb_5Ge_3O_{11}$: Fe^{3+} crystals in the bromine-containing atmosphere, there appear new satellites of comparable intensity (marked by arrows in Fig. 2, spectrum *c*). Like the signals of Fe^{3+}–Cl^- complexes, these satellites split into three components under the deviation of the magnetic field from $\mathbf{B} \parallel \mathbf{C}_3$. It reasonable to attribute these satellites to the transitions of three dimer triclinic Fe^{3+}–Br^- com-

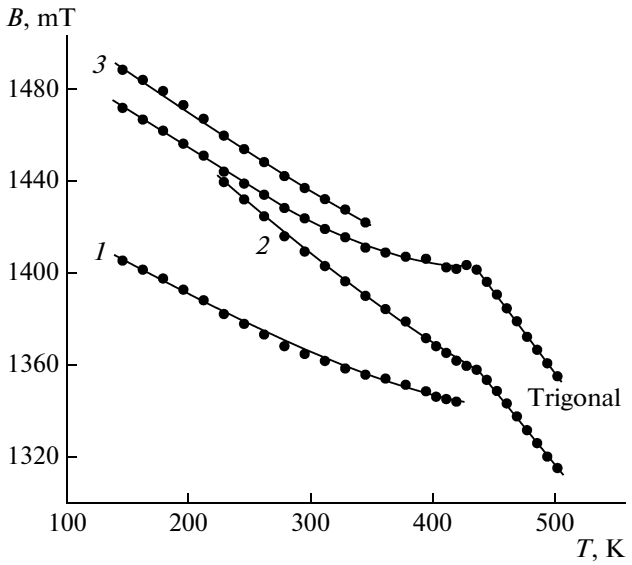

Fig. 3. Temperature dependences of the positions of the transition 5 ⟷ 6 of the trigonal center and (*1–3*) satellites with the increasing intensity after annealing in the chlorine-containing atmosphere. $\mathbf{B} \parallel \mathbf{C}_3$, the frequency is 9450 MHz.

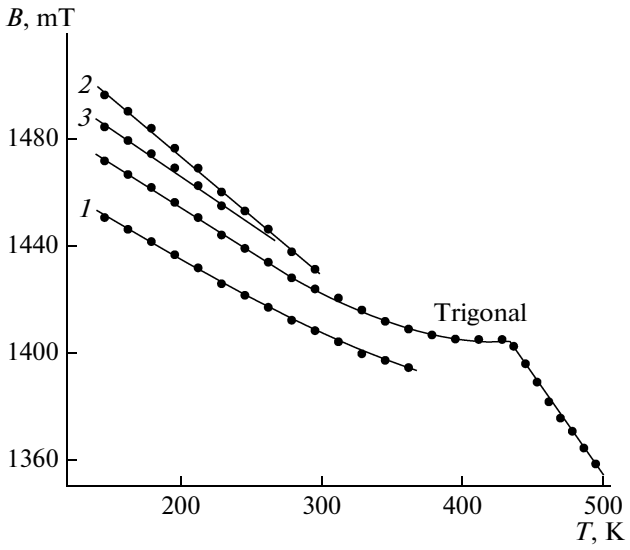

Fig. 4. Temperature dependences of the resonance positions of the transition 5 ⟷ 6 of the trigonal center Fe^{3+} and (*1–3*) satellites formed after annealing of the sample with teflon. $\mathbf{B} \parallel \mathbf{C}_3$, the frequency is 9450 MHz.

plexes, in which the bromine ions are situated in the channels and the paramagnetic ion is in the position Pb7. The values of the second-rank axial parameters of the zero field splitting of these complexes and their difference from b_{20} of the trigonal center are listed in Table 2. Higher values of Δb_{20} than those found for the Fe^{3+}–Cl^- complexes are caused by a noticeable increase in the effective ionic radius of the charge-compensating halogen.

After annealing lead germanate in the presence of teflon, there appear several signals near the transition of the trigonal Fe^{3+} center (Fig. 2, spectrum *d*); the positions of two of them almost coincide at room temperature (Fig. 4). Satellite *2* in spectrum *b* and satellite *1* in spectrum *d* (Fig. 2) appear in nearly the same field but the temperature measurements (Figs. 3 and 4) indicate that these signals belong to different paramagnetic complexes. Like in the case of Fe^{3+}–Cl^- centers, the temperature of the structural transition decreases (Fig. 4) and all EPR signals exhibit strong broadening with an increase in temperature. It should be mentioned that the satellite marked by the tilted arrow and growing under annealing of the samples with teflon (Fig. 2) looses intensity considerably as a result of annealing with a low pressure of oxygen.

Naturally (owing to the charge impurity), weak signals of the Fe^{3+}–Cl^- complexes are seen in the spectrum of the bromine and fluorine-doped samples. In addition, weak signals, whose intensity does not depend on the type of performed annealing, can be noticed for all crystals under investigation (e.g., in a field of 1436 mT). Most probably, these signals repre-

Table 1. Parameters of the spin Hamiltonian of the triclinic complexes Fe^{3+}–Cl^- in lead germanate ($T = 170$ K, the standard deviation *S* and the parameters are given in megahertz; Δb_{20} is the difference between the parameters b_{20} of the triclinic and trigonal centers)

Parameter	Trigonal center	*C*(Cl)-1	*C*(Cl)-2	*C*(Cl)-3
b_{20}	−25320(11)	−24233(11)	−25142(15)	−25342(13)
Δb_{20}		1087	178	−22
b_{21}		−680(100)	210(100)	−500(100)
b_{22}		416(18)	1025(12)	1072(13)
c_{21}		−20(100)	−200(100)	30(100)
c_{22}		15(18)	−1053(12)	−21(13)
S	63	68	69	75
$b_{22\max}$		416	1470	1072

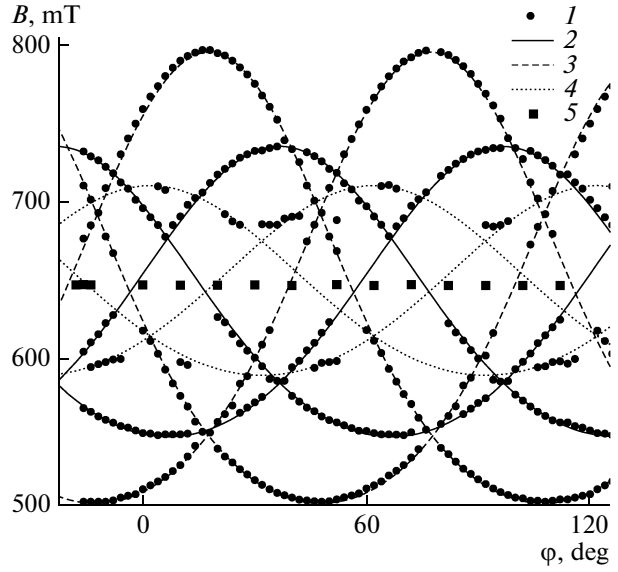

Fig. 5. Azimuthal angular dependences ($\mathbf{B} \perp \mathbf{C}_3$, 170 K) of the positions of the transitions 3 ⟷ 4 of the triclinic Fe^{3+} complexes formed after annealing with teflon, at a frequency of 9447 MHz, according to (*1*) experiment and (*2–4*) calculation for (*2*) *C*(O)-1, (*3*) *C*(O)-2, and (*4*) *C*(O)-3. Symbols *5* indicate the experimental positions of the intense signal of the trigonal center in a field of 648 mT.

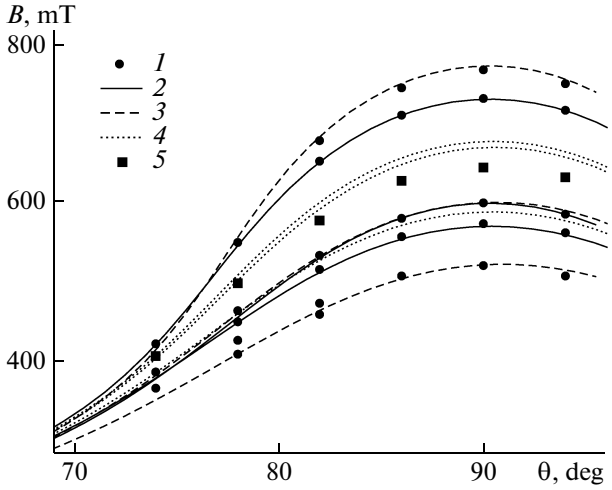

Fig. 6. Angular dependences (in the *ZY* plane at 170 K) of the positions of the transitions 3 ⟷ 4 of triclinic Fe^{3+} centers formed after annealing with teflon according to (*1*) experiment and (*2–4*) calculation for (*2*) *C*(O)-1, (*3*) *C*(O)-2, and (*4*) *C*(O)-3. Symbols *5* indicate the experimental positions of the intense signal of the trigonal center.

sent the transitions of iron centers with other mechanisms of local charge compensation (e.g., association with a lead vacancy).

The spectra of intense complexes, whose transitions in Fig. 2, curve *d* are marked by vertical arrows, were studied in detail. Fragments of the azimuthal and polar angular dependences of the resonance positions of the transitions indicating the triclinic symmetry of these centers are shown in Figs. 5 and 6. The results of the optimization of the second-rank fine-structure parameters of Hamiltonian (1) (under the assumption of the isotropic $g = 2.00$) by minimizing the root-mean square deviation of the calculated transition frequencies from the experimental ones are presented in Table 3. Large values of the root-mean square deviation and errors of the parameters b_{21} and c_{21} of the complex *C*(O)-3 are caused by the fact that the signals of this complex overlap with intense transitions of trigonal or other triclinic centers for significant part of orientations (Figs. 5 and 6).

4. Similar to the complexes Fe^{3+}–Cl^- and Fe^{3+}–Br^-, the spectra that appear under annealing in the fluorine atmosphere could be attributed to the dimer centers Fe^{3+}–F^-. However, Bush and Venevtsev [9] concluded from their X-ray diffraction and spectroscopic investigations of lead germanate crystals grown with a fluorine impurity that F^- ions substitute O^{2-} with the formation of the required number lead defects. In the case of doping the samples by fluorine from the gas phase, the substituted oxygen ions most probably fall into empty channels of the structure and become partly associated with trivalent iron ions. The existence of oxygen ions even in the channels of pure lead germanate is permitted in [10].

In fact, Gd^{3+} complexes with a large zero field splitting and the principal magnetic axis perpendicular to C_3 were discovered in gadolinium-doped lead germanate annealed in the fluorine-containing atmosphere and attributed to the dimer Gd^{3+}–F^- centers

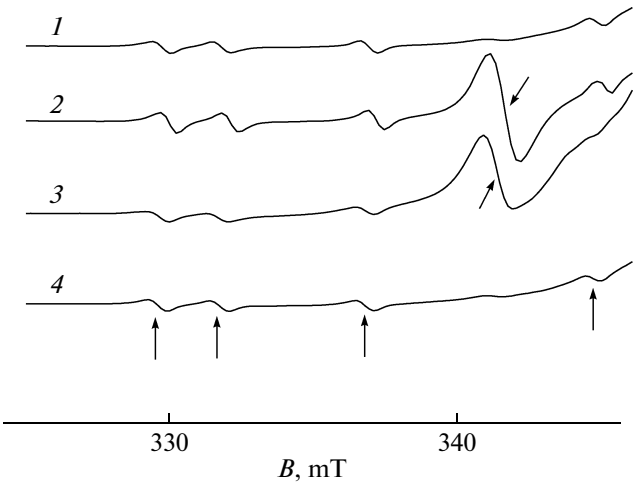

Fig. 7. Fragment of the EPR spectrum with the signals of Mn^{2+} (vertical arrows) and Cu^{2+} (tilted arrows) in the field $\mathbf{B} \parallel \mathbf{C}_3$ at room temperature in the low-field wing of the transition 5 ⟷ 6 of the trigonal center Fe^{3+} for (*1*) initial sample and (*2*) after annealing in the bromine-containing atmosphere, (*3*) after annealing with $ZnCl_2$, and (*4*) after annealing with teflon.

with the fluorine ions in the position of one of the nearest O^{2-} ions [11]. The Gd^{3+}–O^{2-} complexes in the same crystals with the oxygen ions localized in the channel interstices were studied in [12]. The specific feature of their EPR spectra is a considerable increase in intensity after annealing the samples grown at a low pressure of oxygen in air [12]. In our opinion, there are no grounds to assume that the presence of trivalent iron or gadolinium ions in lead germanate affects noticeably on the character of defect formation under doping by halogens.

Another argument in favor of the hypothesis that annealing of $Pb_5Ge_3O_{11}$ with fluorine leads to the appearance of other defects than annealing in chlorine or bromine-containing atmosphere is the effect of the above annealings on the EPR spectra of bivalent copper. The presence of copper and manganese in the lead germanate samples is caused by impurity of lead oxide used in the synthesis. Figure 7 presents the fragment of the EPR spectra with weak signals of triclinic Cu^{2+} complexes [13, 14] and a trigonal Mn^{2+} center [15] in the low-field wing of the intense transition of Fe^{3+}. The nonequidistance of four low-field components (two high-field ones are buried behind the intense signal of Fe^{3+}) of the hyperfine structure of the transition $1/2 \leftrightarrow -1/2$ of Mn^{2+} are caused by a close crossing of the electron levels $-1/2$ and $3/2$ [15]. As is seen in Fig. 7, annealing of the crystal with zinc chloride or cesium bromide leads to the appearance or a strong increase in the intensity of the signal of Cu^{2+}, whereas annealing with teflon makes no effect.

Based on the above results, it can be concluded that the triclinic complexes C(O)-1, C(O)-2, C(O)-3 are the dimers Fe^{3+}–O^{2-}, whose oxygen ions are situated in the interstitial channels of the structure and the Fe^{3+} ion is localized in the position Pb7. The latter statement is based on the closeness of the diagonal fine-structure parameters of the trigonal and triclinic centers.

The temperature behavior of the resonance position $B_{res}(T)$ of the transition $5 \leftrightarrow 6$ ($1/2 \leftrightarrow 3/2$) of the trigonal center Fe^{3+} (Figs. 3 and 4) in the paraelectric phase in $\mathbf{B} \parallel \mathbf{C}_3$ is caused by the linear dependence of the zero field splitting parameter b_{20} on temperature. The mechanisms of this dependence are thermal expansion of the crystal and the spin–phonon interaction [16], which most probably weakly change under the second-order phase transition. The positions of the transitions of the triclinic complexes Fe^{3+} at $\mathbf{B} \parallel \mathbf{C}_3$ also contain weak contributions quadratic in the parameters b_{22}, c_{22}, b_{21}, and c_{21}, which can be neglected.

In the ferroelectric phase, there appears the contribution $\Delta b_{20}(P)$ to b_{20} associated with spontaneous polarization. Expanding $\Delta b_{20}(P)$ in powers of P we find for the paramagnetic center, which has the symmetry plane $\sigma_h \perp C_3$ in the paraelectric phase,

$$\Delta b_{20}(P) = mP^2 + nP^4 + \ldots. \quad (2)$$

Table 2. Diagonal parameters of the spin Hamiltonian of the triclinic centers Fe^{3+}–Br^- in lead germanate (T = 300 K, all the parameters are given in megahertz; Δb_{20} is the difference between the parameters b_{20} of the triclinic and trigonal centers)

Parameter	Trigonal center	C(Br)-1	C(Br)-2	C(Br)-3
b_{20}	−24670(20)	−23560	−24240	−24805
Δb_{20}		1110	430	−135

Table 3. Parameters of the spin Hamiltonian of the triclinic complexes of Fe^{3+} in lead germanate annealed in the fluorine-containing atmosphere (T = 170 K, the standard deviation S and all the parameters are given in megahertz, n is the number of experimental fields included in the fit, and Δb_{20} is the difference between the parameters b_{20} of the triclinic and trigonal centers)

Parameter	C(O)-1	C(O)-2	C(O)-3
b_{20}	−24983(20)	−25613(20)	−25460(20)
Δb_{20}	337	−293	−140
b_{21}	−210(250)	−40(300)	−200(900)
b_{22}	−1534(12)	2013(15)	1021(15)
c_{21}	400(200)	−1140(240)	150(650)
c_{22}	−364(15)	1389(12)	67(20)
n	101	113	52
S	70	90	98
$b_{22\max}$	1577	2445	1023

The nonlinearity of temperature dependence of $B_{res}(T)$ and, consequently, of $b_{20}(T)$ of the trigonal center in the ferroelectric phase is due to a considerable value of the second term in Eq. (2) and to the deviation of the behavior of the order parameter in lead germanate [17, 18] from the dependence

$$P^2 \sim (T_0 - T) \quad (3)$$

(T_0 is the temperature of the structural transition) typical for second-order phase transitions. For the centers, which do not have the symmetry plane $\sigma_h \perp C_3$ in the paraelectric phase, the contribution $\Delta b_{20}(P)$ includes both odd and even powers of P; consequently, these complexes should exhibit dissimilar behavior of $B_{res}(T)$. In this case, there exist two nonequivalent centers (opposite signs of the odd powers of P) in the ferroelectric phase, whose spectra coincide in the paraelectric phase at $\mathbf{B} \parallel \mathbf{C}_3$. If the compensating ion can move along the channel, the intensities of these spectra in the ferroelectric phase can differ considerably.

Taking into account the aforesaid, the triclinic complexes C(Cl)-1, C(Cl)-3, C(O)-1, and C(O)-3, which exhibit the temperature behavior similar to that of the trigonal center, should be attributed to nearly

monoclinic centers with the charge-compensating ion located in the channel near the reflection plane of the paraelectric phase. On the other hand, the centers C(Cl)-2 and C(O)-2 should be regarded as the complexes, in which the compensation effect is displaced considerably from the mirror plane.

At the same time, taking into account that $b_{22\max}$ of triclinic centers depends on the coordinates of the charge-compensating defect as $3\sin^2\theta\cos 2\varphi$ [19] and assuming that halogen and oxygen ions of the complexes under investigation are situated only in the nearest channel (at a distance of 0.59 nm), the dipolar complexes C(Cl)-2 and C(O)-2 having the maximum values of $b_{22\max}$ should be thought of as located most closely to the reflection plane of the paraelectric phase. Obviously, this contradicts with the conclusions drawn from the temperature behavior of the triclinic spectra.

The specific feature of the C(Cl)-1 and C(Br)-1 complexes is a large difference between their values of b_{20} and the corresponding value for the trigonal center. The maximum value of $|\Delta b_{20}|$ should be expected for the complexes, whose compensating defect is situated in the mirror plane ($\theta = 90°$). The sign of this shift in the superposition model depends on the sign of the intrinsic parameter $\bar{b}_2(R_0)$ in the expression [19]

$$b_{20} = \sum_d K_{20}(\theta_d)\bar{b}_2(R_0)(R_0/R_d)^t, \qquad (4)$$

where $K_{20}(\theta_d) = (1/2)(3\cos^2\theta_d - 1)$ is the angular structure factor, R_d and θ_d are the spherical coordinates of ligands.

The values of the intrinsic parameters ($\bar{b}_2(R_0)$ and t) for the Fe^{3+} ion in the Cl or Br surrounding are unavailable in literature. The parameter $\bar{b}_2(R_0)$ in a number of studied oxide and fluoride compounds is negative and the exponent is $t \approx 8$ [19]. Using the structural data for lead germanate in the para- and ferroelectric phase [4, 6] and the corresponding values of b_{20} of the trigonal Fe^{3+} center we found the following intrinsic parameters of the model for six-fold oxygen surrounding: $\bar{b}_2(R_0) \approx -2.34\ \text{cm}^{-1}$, $t \approx 9$, $R_0 = 2.101$ Å. Assuming that the sign of $\bar{b}_2(R_0)$ in chlorides and bromides is also negative, we come to the conclusion that the maximum positive value of Δb_{20} is exhibited by the paramagnetic complex with the compensator situated in the symmetry plane of the paraelectric phase. In the case of the C(Cl)-1 center, this conclusion contradicts with the previous one based on comparison of $b_{22\max}$ values.

It should be mentioned that all the above data on the localization of charge-compensating anions imply the dominance of the direct interaction of the paramagnetic ion with the compensating defect and neglect interaction with the nearest neighborhood relaxed owing to the emergence of this defect. On the other hand, it is obvious that the properties of the paramagnetic center, including the symmetry properties, are largely determined by the nearest ligands. The inclusion of the lattice relaxation owing to both paramagnetic and charge-compensating defects will be the subject of the future work.

ACKNOWLEDGMENTS

This study was supported by the Ural Federal University within the framework of the Competition of Young Scientists and the Program of the Development of the Ural Federal University.

REFERENCES

1. V. A. Vazhenin, A. D. Gorlov, K. M. Zolotareva, A. P. Potapov, A. I. Rokeakh, and Yu. A. Sherstkov, Sov. Phys. Solid State **21** (1), 158 (1979).
2. A. A. Mirzakhanyan, A. K. Petrosyan, and H. R. Asatryan, Phys. Status Solidi B **105**, K55 (1981).
3. G. R. Asatryan, V. A. Vazhenin, A. D. Gorlov, A. A. Mirzakhanyan, and A. P. Potapov, Sov. Phys. Solid State **23** (8), 1442 (1981).
4. Y. Iwata, H. Koizumi, N. Koyano, I. Shibuya, and N. Niizeki, J. Phys. Soc. Jpn. **35**, 314 (1973).
5. V. A. Vazhenin, A. P. Potapov, A. V. Fokin, and M. Yu. Artyomov, Phys. Solid State **54** (5), 2450 (2012).
6. Y. J. Iwata, J. Phys. Soc. Jpn. **43**, 961 (1977).
7. H. Iwasaki, S. Miyazawa, H. Koizumi, K. Sugii, and N. Niizeki, J. Appl. Phys. **43**, 4907 (1972).
8. S. A. Al'tshuler and B. M. Kozyrev, *Electron Paramagnetic Resonance* (Academic, London, 1964; Nauka, Moscow, 1972), p. 121.
9. A. A. Bush and Yu. N. Venevtsev, Izv. Akad. Nauk SSSR, Neorg. Mater. **17**, 302 (1981).
10. V. M. Duda, A. I. Baranov, A. S. Ermakov, and R. C. T. Slade, Phys. Solid State **48** (1), 63 (2006).
11. V. A. Vazhenin, A. N. Ivachev, A. P. Potapov, and M. Yu. Artyomov, Phys. Solid State **53** (10), 2085 (2011).
12. V. A. Vazhenin and K. M. Starichenko, Sov. Phys. Solid State **29** (8), 1459 (1987).
13. V. A. Vazhenin, A. D. Gorlov, A. I. Krotkii, A. P. Potapov, and K. M. Starichenko, Sov. Phys. Solid State **31** (1), 102 (1989).
14. V. A. Vazhenin, A. P. Potapov, V. B. Guseva, and A. D. Gorlov, Phys. Solid State **49** (4), 660 (2007).
15. V. A. Vazhenin, A. D. Gorlov, and A. P. Potapov, Sov. Phys. Solid State **28** (7), 1142 (1986).
16. R. Biederbick, A. Hofstaetter, and A. Sharmann, Phys. Status Solidi B **84**, 449 (1978).
17. V. A. Vazhenin, V. B. Guseva, V. Ya. Shur, E. V. Nikolaeva, and M. Yu. Artemov, Phys. Solid State **43** (10), 1952 (2001).
18. M. P. Trubitsyn, S. Waplak, and Yu. D. Krokhmal, Phase Transitions **80**, 155 (2007).
19. *Crystal Field Handbook*, Ed. by D. J. Newman and Betty Ng (Cambridge University Press, Cambridge, 2000).

Translated by A. Safonov